THE CENTER-TO-LIMB VARIATION OF THE PHOTOSPHERIC WAVE SPECTRUM

M. STIX and H. WÖHL
Universitäts-Sternwarte Göttingen, F.R.G.

(Received 4 March; in revised form 3 April, 1974)

Abstract. Using photoelectric observations in the Fe 5576 Å line we obtained line-of-sight velocities at nine different positions on the solar disk, as functions of one horizontal co-ordinate and time. With the help of the Fast Fourier Transform algorithm we calculated two-dimensional power spectra (horizontal wave number and frequency). Special attention was given to the possible existence of horizontal sound waves. We find only very little power in these waves; thus the excitation of the solar atmosphere to oscillations by locally overshooting granules, which should be accompanied by horizontal sound waves with large amplitudes, can play only a minor role.

1. Introduction

Since the discovery of the oscillatory velocity field in the solar atmosphere many observers measured these oscillations at different positions of the solar disk. For example, both Leighton *et al.* (1962) and Evans and Michard (1962) already found that the oscillations with 200–300 s period are more or less vertical because of their decreasing visibility with increasing distance from the center of the disk. Noyes (1967; see also Deubner, 1971) studied the mean-square line-of-sight velocity as a function of position on the disk and found that the ratio of the horizontal to vertical rms velocities decreases considerably with height in the atmosphere. Howard (1967) showed that the distribution of periods has a pronounced peak close to 300 s at the center of the disk but is much broader near the limb.

For a comparison with theoretical work the most useful information probably is the two-dimensional spectrum (horizontal wave number, k, and frequency, ω). Several observers investigated such 'diagnostic diagrams' by means of two-dimensional power spectra calculated from data obtained at the center of the disk (Mein, 1966; Frazier, 1968; Tanenbaum *et al.*, 1969; Edmonds and Webb, 1972a, b), but only one example (Deubner, 1972) is known to us where a two-dimensional power spectrum has been computed from observations made not at the center of the disk.

There is one particular problem which makes the measurement of two-dimensional spectra near the limb desirable, namely the possible existence of horizontal sound waves (Lamb waves) in the solar atmosphere. If the atmosphere is locally excited to oscillations by overshooting granules, we should expect such waves; in fact, according to calculations of Meyer and Schmidt (1967) and Stix (1970), they should contain most of the energy. Figure 1, taken from Stix's paper, is an example of a theoretical energy distribution: the area of each circle is proportional to the kinetic energy of the mode defined by the k and ω values of the center of that circle. Of course, the vertical velocity

Solar Physics **37** (1974) 63–74.

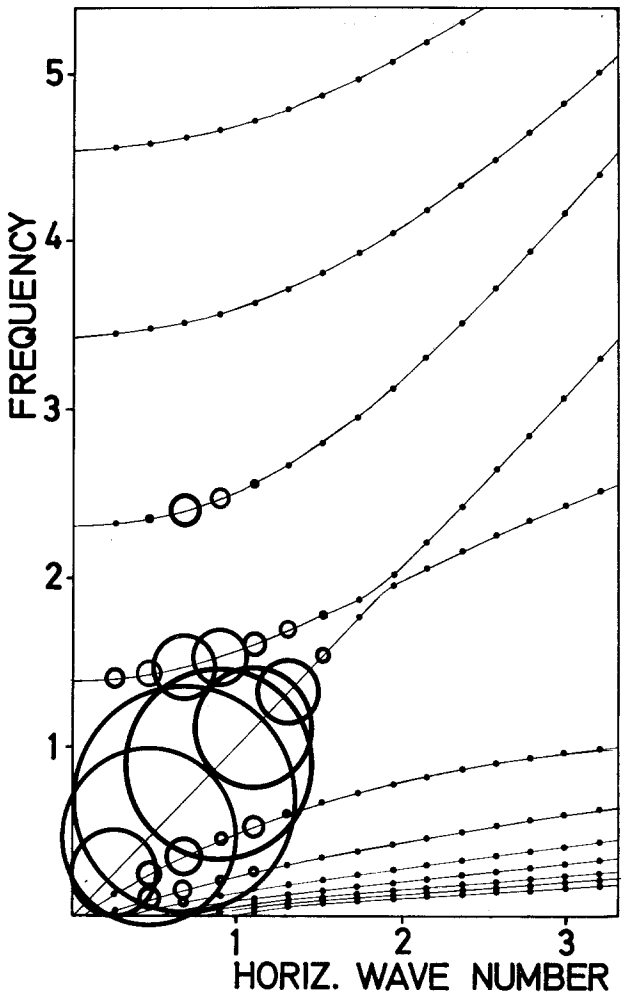

Fig. 1. Theoretical energy distribution in the diagnostic diagram (after Stix, 1970). Wave number and frequency units are $(2H)^{-1}$ and $c/2H$ respectively, where H is the scale height and c the velocity of sound.

component contributes at most a small fraction to this energy, depending on the details of the theoretical model, for example the boundary conditions. Thus the non-existence of horizontal sound waves in power spectra obtained at the disk center is not meaningful. These waves should however appear in off-center power spectra, if at all they do exist on the Sun.

In order to clarify this problem and because of the general importance of two-dimensional power spectra of *all* velocity components we have measured the line-of-sight velocity $v(x, t)$ as a function of one horizontal co-ordinate, x, and time, t, at several positions on the disk. These observations will be reported in Section 2. In Section 3 we describe the computation of the power spectra; the results will be discussed in Section 4.

2. Observations

The data were obtained by one of us (H.W.) at the Institute for Solar Research of the Deutsche Forschungsgemeinschaft at Orselina (Switzerland) during the period June 9 to July 1, 1973. The vacuum telescope (Gregory-Coudé type, 45 cm ⌀, $f=24$ m), which was controlled by a Honeywell H 316 (8 K) computer, made a number of one-dimensional scans on the Sun. The entrance hole of the spectrometer was 2″ in diameter. An interference filter was used to separate the orders and the spectrometer (grating 25 cm long, 300 grooves mm^{-1}) was operated in the 10th order to measure the Doppler shift of the Fe 5576 Å line photoelectrically. This line was chosen because it is magnetically non-split, not very sensitive to temperature fluctuations and in a spectral region where we have the efficiency maximum of our equipment.

Two methods were used to measure the line shift: In one set of measurements the Doppler compensator of the polarimeter (see Wiehr, 1969) was used and one value for the line shift at each point on the Sun was obtained. In the second set of measurements two exit slits were used in order to measure the intensities in the steepest parts of both sides of the line profile. The slit widths corresponded to about 100 mÅ on each side. Two intensity values (one for each side) and a third value proportional to the intensity behind the interference filter (in the 'continuum') were recorded. The Doppler shift is then proportional to the difference of the intensities measured in the sides divided by the 'continuum'-value. (The second method was used because of difficulties we had had in the past with our Doppler compensator. The method will be referred to as 'flank' method, in order to avoid the word 'wing', which would be misleading in this context.)

The computer guided the telescope from the center of the solar disk along the Sun's axis of rotation to a chosen point on the disk. (The angle between the northern extremity of the axis of rotation and the north point of the disk, usually called P, was taken from the astronomical ephemerides. The heliographic latitude, B_0, which was rather small in June 1973 and has less importance for the corrections was not taken into account.) Then the computer controlled the scanning of the Sun from west to east over a length of 176″ in steps of one arcsecond and the collecting of averaged analog-digital converted data of the line shift at each point. When a scan was completed the telescope was guided back to the starting point, the data were written on magnetic tape and, after an automatic correction for the solar rotation, the next scanning cycle started.

The scanning time for one cycle was about 29 s and the total period about 35 s. This value varied by a maximum of 2 s since the correction for the solar rotation is different at different θ values.

The calibrations were obtained by defocussing the image and rotating the grating. This was done within a few seconds over a wavelength region which equaled to Doppler velocities of about ± 2 km s^{-1}. The data collected during the calibrations were written on magnetic tape too.

The data were obtained during periods of rather good seeing with a maximum

blurring of about 3″ and a maximum guiding error of about the same value. The data were collected in fairly inactive solar regions which was checked by observing the scanned regions through Hα- and Ca^+ K-line filters.

We intended to collect the data of 180 cycles for each of the chosen θ values, but, caused by some defects of the magnetic tape unit, this was only possible for about two thirds of the sets of scans (see Table I).

In Table I several parameters of the scans are presented. Figure 2 shows examples of parts of two sets of data.

TABLE I

Census of the data

Date	Measuring method	θ	Number of scans	Observing conditions
9 June 1973	flanks	0°	180	good seeing
11 June 1973	flanks	15°	180	good seeing
12 June 1973	flanks	30°	180	good seeing
10 June 1973	flanks	50°	109	good seeing
10 June 1973	flanks	60°	180	good seeing
12 June 1973	flanks	65°	180	good seeing
11 June 1973	flanks	70°	180	good seeing
11 June 1973	flanks	75°	88	good seeing
30 June 1973	flanks	0°	180	good seeing, some clouds
1 July 1973	Doppler	0°	180	good seeing
13 June 1973	Doppler	15°	180	some cirrus
14 June 1973	Doppler	30°	92	good seeing
14 June 1973	Doppler	40°	180	some clouds
24 June 1973	Doppler	50°	180	some clouds
25 June 1973	Doppler	60°	173	good seeing
25 June 1973	Doppler	65°	139	good seeing
25 June 1973	Doppler	70°	36	good seeing
25 June 1973	Doppler	75°	96	good seeing

3. Two-Dimensional Fourier Analysis

The numerical analysis described below was carried out by one of the authors (M.S.) with the help of the Fast Fourier Transform algorithm and an UNIVAC 1108 computer.

When converted from Doppler shift to velocity, each set of our data consists of a matrix v_{jl}, where v_{jl} denotes the line-of-sight velocity at the j-th point of the l-th scan. We computed the Fourier transform of v_{jl} in two steps: the space domain was first transformed into the wavenumber domain; the result of this operation, which still depended on time, was then for each wave number transformed into the frequency-wave number domain. Brault and White (1971) and Edmonds and Webb (1972a) recently have emphasized the advantages of the Fast Fourier Transform algorithm for the reduction of observational data like ours. We therefore restrict ourselves to a brief description of the single steps of the analysis.

Prior to the Fourier transformation the data were modified by two operations: for

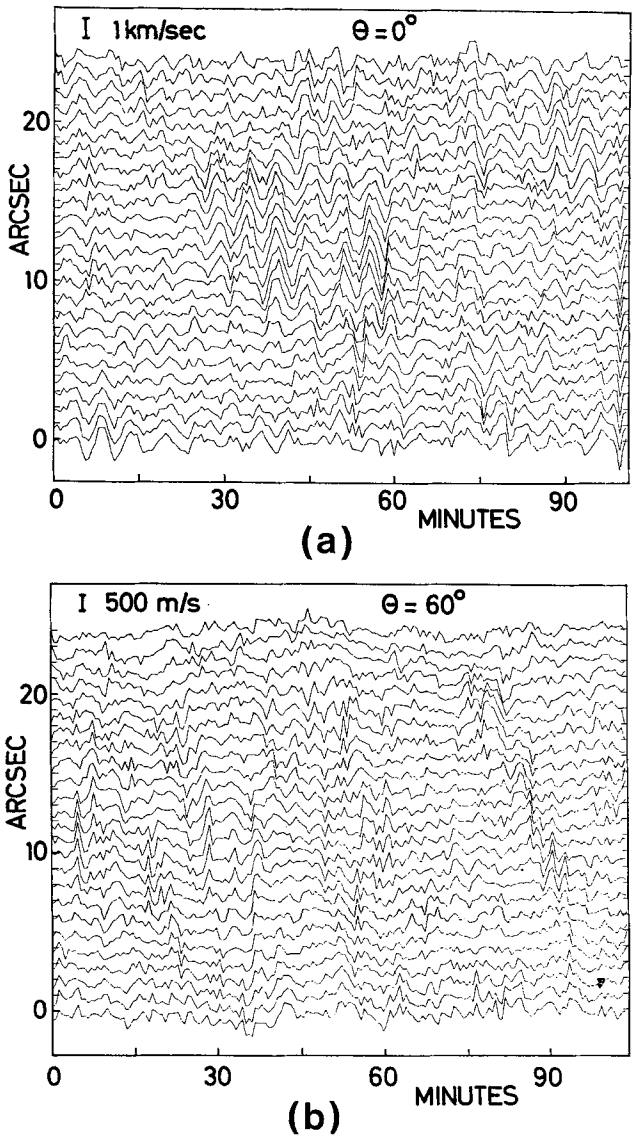

Fig. 2a–b. Line-of-sight velocity at two positions on the disk, as a function of time and one horizontal co-ordinate.

both fixed j and l, the individual averages and linear trends were first removed from v_{jl}. Low-frequency and small-wave number spikes in the spectrum are avoided in this way and the effect of redistribution of these spikes by the resolution function is thus reduced. The first and last 10% (both in space and time) of these new velocity values were then multiplied by a cosine bell apodization function. This 'end region masking' apodizes the side lobes of the resolution function; it therefore further reduces the spectral redistribution.

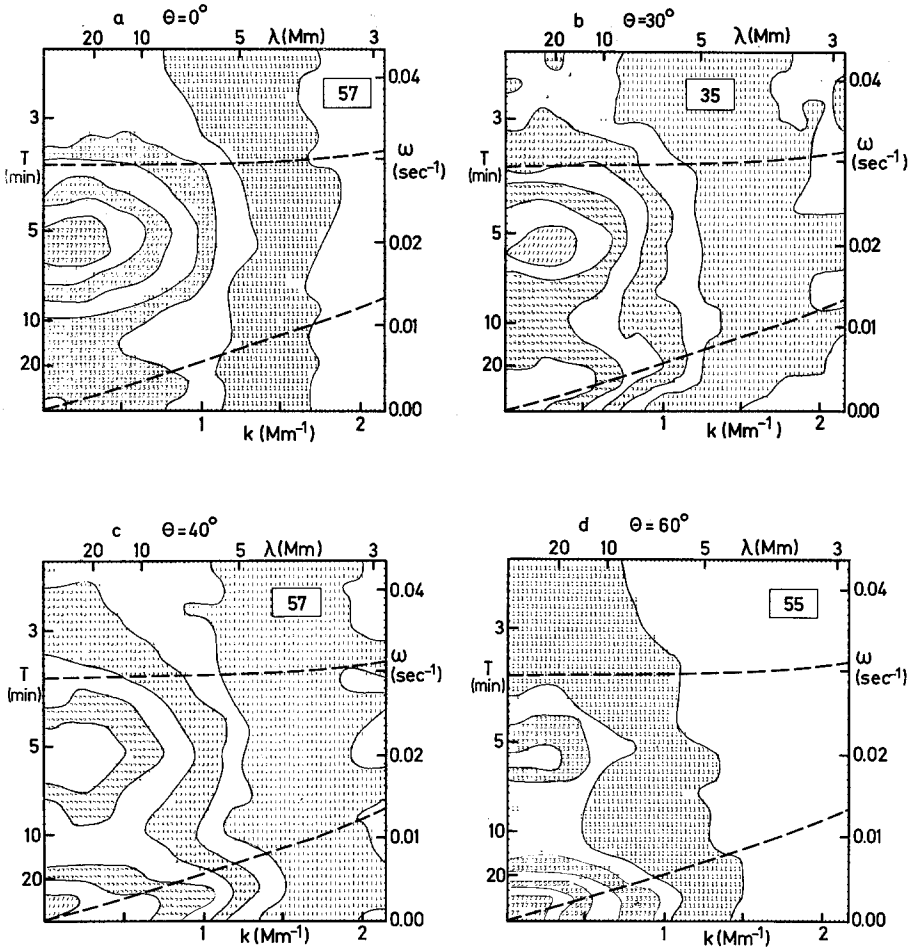

Fig. 3a–d. Normalized power spectra calculated from Doppler compensator measurements. The contours mark the 0.5, 2, 4, 8, 16, 32 and 64% levels; every other interval between these levels is shaded. The lower dashed line is the locus of horizontal sound waves, the upper is the acoustic cut-off frequency. T and λ are period and horizontal wave length respectively.

Since our data are real, the first step of the Fourier transformation leads to a transform which has conjugate symmetry in the wave number domain. But this transform is generally complex so that the two-dimensional transform is *not* symmetric, although it has point-symmetry with respect to the origin. In order to study a complete power spectrum one should therefore consider at least two quadrants of the $k-\omega$ plane (Mein, 1966; Edmonds and Webb, 1972a, b). In this way the waves propagating forward and backward along the scanning direction on the Sun are separated. In our investigation we were however not interested in distinguishing between these two possibilities. Our power spectra were therefore computed according to

$$P(k_j, \omega_l) = 2(|f(k_j, \omega_l)|^2 + |f(k_j, -\omega_l)|^2),$$

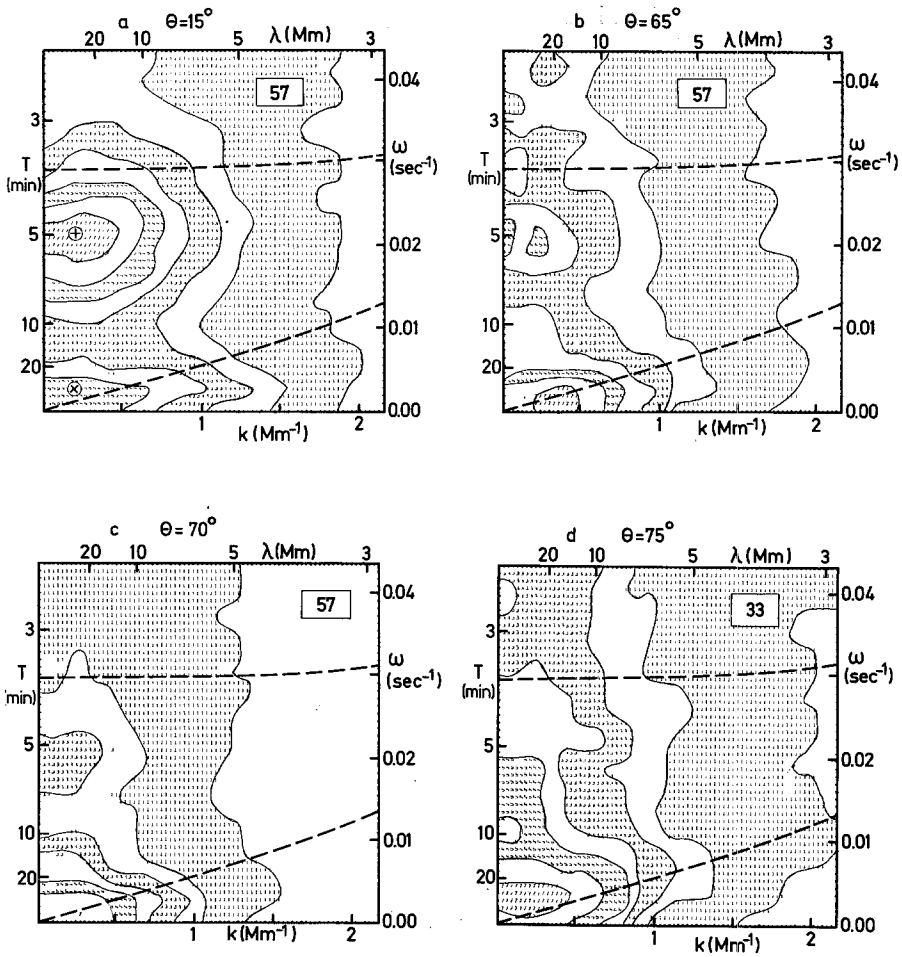

Fig. 4a–d. Normalized power spectra calculated from flank measurements. Legend as in Figure 3.

where k_j and ω_l denote the j-th wave number and l-th frequency, and f is the (complex) two-dimensional Fourier transform.

In order to improve the statistical stability the power spectra were smoothed by averaging over 5 by 5 (5 by 3 when the total number of scans was less than 128) spectral points. This lowers the spectral resolution considerably, but we are only interested in the mean power spectrum and not in the multiple peaks occuring in raw spectra, which in any case are unstable in time (Howard, 1967; White and Cha, 1973) and space (Deubner, 1972; 1973). The reliability of such smoot hedspectra can be estimated from the number, D, of equivalent degrees of freedom, i.e. essentially the number of harmonics contributing to each (smoothed) spectral value. The value of D was calculated according to Equation (12) of Edmonds and Webb (1972a) and is stated in the rectangle in each of the power spectra shown in Figures 3 and 4. Using Figure 6 of Edmonds (1966), we may obtain 50% lower and upper confidence limits; in the most unfavourable case, $D=33$, these

are given by factors 0.87 and 1.20 respectively (for $D=57$ we obtain 0.89 and 1.14). Edmonds (1966) discussed influences which possibly reduce the magnitude of D by a certain amount, but in view of the small variation of the confidence limits in the range above, say, $D=30$ we did not further study this problem. For the same reason there is little gain in confidence by increasing D further, i.e. it is useless to take more than 5 by 5 points for the averaging. We did however check the stability of our spectra by another method: since for computational reasons, we used only 128 out of the 176 velocity values of each scan to compute the space transform, we had the possibility of selecting various (overlapping) segments of 128 points and thus of computing several power spectra from each of our velocity matrices v_{jl}. These spectra showed little variation. The size of the rectangle containing D indicates the spectral resolution after smoothing.

The observational limitations in the $k-\omega$ plane are given by the total length and duration of the observations and by the Nyquist wave number and frequency, viz.

$$\frac{2\pi}{128''} < k < \frac{\pi}{2''}$$

$$\frac{2\pi}{N_s DT} < \omega < \frac{\pi}{DT},$$

Where N_s is the number of scans (see Table I) and DT is the scanning period (≈ 35 s). The factor $\frac{1}{2}$ in the upper wave number limit obtains from the 2″ aperture used in the observations. Of course, the seeing in effect further reduces this limit. Also, as a consequence of the removal of linear trends, the lower frequency and wave number limits must be multiplied at least with a factor 2.

The final step in the calculation was an interpolation for a common frequency scale. This was necessary because of the different scanning periods at different disk positions, θ, as mentioned in Section 2.

It should be kept in mind that the spectra obtained in the way described here are not true diagnostic diagrams since they are based on spatially one-dimensional observations. Thus $k=k_x$ is a spatially one-dimensional wave number, and not the total horizontal wave number $k_h=(k_x^2+k_y^2)^{1/2}$. One correct method would be to measure the velocity repeatedly within a two-dimensional array on the Sun and then to compute the Fourier transform in two space co-ordinates and time. The method employed in the present paper certainly overestimates the power at small wave numbers. We have checked this effect by computing $k_j P(k_j, \omega_l)$ for one of our spectra (as proposed by Deubner, private communication). This probably brings the power at small k closer to the truth, but the major features of the spectra remain unchanged. On the other hand, unwanted power is produced at large wave numbers; for example, the 1% level is shifted from $k\approx 2$ Mm^{-1} to $k\approx 3$ Mm^{-1}. Of course, another method to obtain true diagnostic diagrams is the computation of the autocorrelation function and its Hankel transform. But this method, too, has its difficulties; the occurrence of negative power is one of them. For all these reasons we decided to present only power

spectra computed in the way described in the first paragraphs of this section. For a 128×256 matrix the calculation of such a spectrum took only about 30 s.

There is only little difference between the normalized power spectra calculated from Doppler compensator and flank measurements at the same θ. Thus the eight examples shown in Figures 3 and 4 sufficiently describe our results. These results will be discussed in the following section.

4. Discussion

The most conspicuous feature in Figures 3 and 4 is the peak at small wave numbers and ca. 5 min period. As expected, this peak is most important at small θ values, whereas for θ larger than, say, 40° the low-frequency ridge extending over a wide wave number range becomes dominant. Also as expected, the five-min peak lies in the region of evanescent waves, i.e. the region below the acoustic cut-off frequency (upper dashed curve, according to calculations of Schmidt and Stix, 1973) and above the high-frequency limit for internal gravity waves which, for the relatively small wave numbers considered here, approximately coincides with the horizontal sound wave curve (lower dashed curve). Thus our power spectra confirm the theory that the five-min oscillations are forced oscillations coupled to subphotospheric eigenmodes (Ulrich, 1970; Leibacher, 1971).

Figure 5 shows the center-to-limb variation of the two spectrum points at $\lambda = 31.0$ Mm, $T = 298$ s (a; + in Figure 4a) and $\lambda = 31.0$ Mm, $T = 38.5$ min (b; × in Figure 4a). The former typically represents the five-min oscillation. The points scatter around a $\cos^2\theta$ curve, indicating once more the vertical character of this oscillation. The situation is less clear for the low-frequency band (Figure 5b): although its variation resembles a $\sin^2\theta$ curve for small and moderate θ values, thus suggesting a horizontal flow, the power becomes again smaller in the vicinity of the limb. A similar effect was found by Deubner (1971) in some of his 'stationary' velocities. He argues that the decrease toward the limb is caused by the decreasing spatial resolution. Another possible explanation is that the magnitude of the horizontal motion decreases with height in the solar atmosphere; we observe this decrease as we approach the limb because the optical depth varies approximately like $\cos\theta$. In fact, Deubner suggests such a height dependence from his results obtained from lines originating at different levels.

It should be kept in mind that there is no isolated peak near 38.5 min. We have chosen this period since it is representative for the low-frequency ridge in our power spectra (other points within this ridge show essentially the same behaviour) but still sufficiently short to be unaffected by the removal of the linear trends from the data. We anticipate that the low-frequency ridge is part of a continuum extending to much lower frequencies. The wave lengths are consistent with the scale of the supergranulation; the variation in time may be caused by supergranulation boundaries moving back and forth along the scanned line on the Sun.

Figure 5 also indicates that the power obtained from Doppler compensator observations is slightly smaller than the power obtained from flank measurements. We

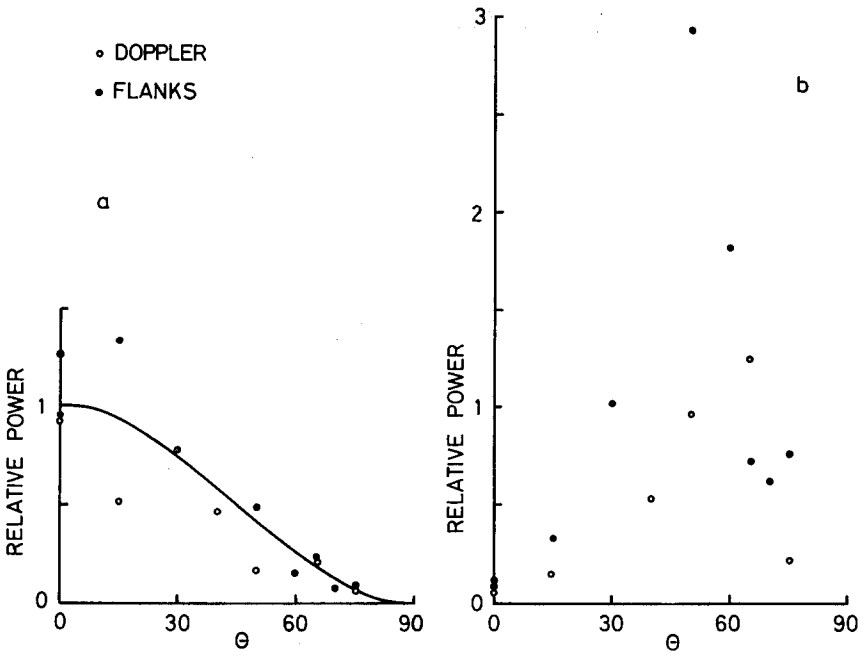

Fig. 5a–b. Center-to-limb variation of the power at the two points marked in Figure 4a by + (a) and × (b). The wave length is 31.0 Mm in both cases, the periods are 298 s and 38.5 min. The solid curve is a $\cos^2\theta$ curve, the amplitude of which is fitted by least-squares and then normalized to unity.

have considered several possible sources of this difference (which is also present in the original data). First, the two methods utilize the same part of the line profile only when $v=0$. In the case $v\neq 0$ the flank measurements are made at slightly different positions than the corresponding Doppler measurements. Since the various portions of the line profile originate in different heights in the atmosphere this could lead to different results if the velocity varies with height. Such an effect makes however little sense in our case: It is known that the amplitude of the five-min oscillation increases with increasing height (Noyes, 1967), whereas the horizontal supergranular flow decreases (see the above remark). On the other hand both Figures 5a and 5b show *smaller* Doppler values. Secondly, calibration errors in the flank method due to the non-linearity of the line profile also seem improbable since both the calibration and the measurements themselves are well within the linear portion of the profile. A third possibility is the inertia of the Doppler compensator. But this argument, too, seems to be inconclusive since we would expect deviations in both directions. Thus the situation remains somewhat unclear; but, fortunately, there are no consequences as far as the *relative* distribution of power is concerned. In three cases we had difficulties calibrating Doppler measurements; these were omitted from Figure 5. The normalization of all power values was corrected for the varying number of scans.

A second very conspicuous result is the large difference of Figure 1 and Figures 3 and 4 as far as the horizontal sound waves are concerned. Although a direct compari-

son of an energy spectrum with power spectra is not possible, horizontal sound waves should appear in the power spectrum whenever the observations stem from a layer which is not too high in the atmosphere. The relevant part of the Fe 5576 line profile originates below $\tau \approx 0.1$ so this condition seems to be satisfied. Another problem in predicting horizontal sound waves from theoretical models is the large influence of the boundary conditions. For one thing, the absence of plane-parallel boundaries in the solar atmosphere can destroy the simple wave character of the eigenmodes. Secondly, in the model Figure 1 is based on (Stix, 1970), the overshooting granule is represented by a 'monopole source', i.e. a local rising of the lower boundary. Compressional modes naturally are most sensitive to a perturbation of this type. On the other hand horizontally propagating waves were still present in the later calculations of Schmidt and Stix (1973) where a rising source surrounded by a circular sink was used (so that the net mass flux through the boundary was zero). Thus, we conclude that *horizontal sound waves in the solar atmosphere are less important than we would expect from a theory attributing the solar oscillations predominantly to local excitation by granules.* To be sure, there *are* observed examples of local excitation. Deubner (1974) reported one which very nicely fits to Figure 3 of Schmidt and Stix (1973). In fact, the protrusion of the contour lines along the lower dashed curve of, for example, Figure 4d may by interpreted as horizontal sound waves. But the effect is small, and entirely absent in several other examples.

Acknowledgements

We wish to thank our collegues at the Universitäts-Sternwarte Göttingen, in particular Prof. E. H. Schröter and Dr E. Wiehr, for many stimulating discussions. Dr F.-L. Deubner also contributed very helpful comments. The observations were made at the Institute for Solar Research of the Deutsche Forschungsgemeinschaft at Locarno-Orselina; and the numerical calculations were carried out at the computing center of the Gesellschaft für wissenschaftliche Datenverarbeitung, Göttingen. We thank Dr O. R. White of the High Altitude Observatory, Boulder, Colo., who made the Fast Fourier Transform routine available to us.

References

Brault, J. W. and White, O. R.: 1971, *Astron. Astrophys.* **13**, 169.
Deubner, F.-L.: 1971, *Solar Phys.* **17**, 6.
Deubner, F.-L.: 1972, *Solar Phys.* **22**, 263.
Deubner, F.-L.: 1973, *Solar Phys.* **23**, 304.
Deubner, F.-L.: 1974, in R. Grant Athay (ed.), 'Chromospheric Fine Structure', *IAU Symp.* **56**, (in press).
Edmonds, F. N., Jr.: 1966, *Astrophys. J.* **144**, 733.
Edmonds, F. N., Jr. and Webb, C. J.: 1972a, *Solar Phys.* **22**, 276.
Edmonds, F. N., Jr. and Webb, C. J.: 1972b, *Solar Phys.* **25**, 44.
Evans, J. W. and Michard, R.: 1962, *Astrophys. J.* **136**, 493.
Frazier, E. N.: 1968, *Z. Astrophys.* **68**, 345.
Howard, R.: 1967, *Solar Phys.* **2**, 3.
Leibacher, J. W.: 1971, Thesis, Harvard University.
Leighton, R. B., Noyes, R. W., and Simon, G. W.: 1962, *Astrophys. J.* **135**, 474.

Mein, P.: 1966, *Ann. Astrophys.* **29**, 153.
Meyer, F. and Schmidt, H. U.: 1967, *Z. Astrophys.* **65**, 274.
Noyes, R. W.: 1967, in R. N. Thomas (ed.), 'Aerodynamic Phenomena in Stellar Atmospheres', *IAU Symp.* **28**, 293.
Schmidt, H. U. and Stix, M.: 1973, *Mitteilungen Astron. Ges.* **32**, 182.
Stix, M.: 1970, *Astron. Astrophys.* **4**, 189.
Tanenbaum, A. S., Wilcox, J. M., Frazier, E. N., and Howard, R.: 1969, *Solar Phys.* **9**, 328.
Ulrich, R. K.: 1970, *Astrophys. J.* **162**, 993.
White, O. R. and Cha, M. Y.: 1973, *Solar Phys.* **31**, 23.
Wiehr, E.: 1969, *Solar Phys.* **9**, 225.